Accepted Manuscript

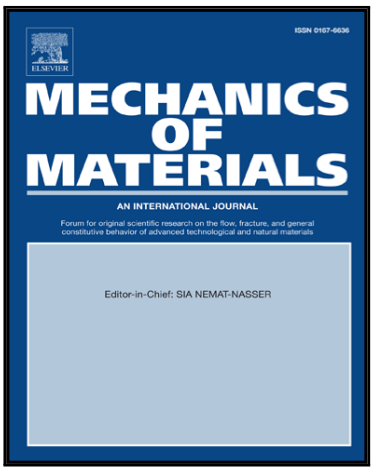

Constitutive equation for the hot deformation behavior of C_{sf}/AZ91D composites and its validity for numerical simulation

Zhenjun Wang , Lehua Qi , Gui Wang , Hejun Li , Matthew S. Dargusch

PII: S0167-6636(16)30234-4
DOI: 10.1016/j.mechmat.2016.08.011
Reference: MECMAT 2634

To appear in: *Mechanics of Materials*

Received date: 19 September 2015
Revised date: 8 July 2016
Accepted date: 16 August 2016

Please cite this article as: Zhenjun Wang , Lehua Qi , Gui Wang , Hejun Li , Matthew S. Dargusch , Constitutive equation for the hot deformation behavior of C_{sf}/AZ91D composites and its validity for numerical simulation, *Mechanics of Materials* (2016), doi: 10.1016/j.mechmat.2016.08.011

Highlights

- The flow stress depends largely on strain besides on temperature and strain rate.
- The model can formulate the flow stress-strain behaviors accurately.
- The FEM results based on the model agree well with the experimental ones.
- The model is valid for FE analysis on the current hot forming of the composites.

Constitutive equation for the hot deformation behavior of C_{sf}/AZ91D composites and its validity for numerical simulation

Zhenjun Wang [a, b, c*], Lehua Qi[b] , Gui Wang [c], Hejun Li [b] , Matthew S. Dargusch [c]

[a] National Defense Key Discipline Laboratory of Light Alloy Processing Science and Technology, Nanchang Hangkong University, Nanchang 330063, China

[b] State Key Laboratory of Solidification Processing, Northwestern Polytechnical University, Xi'an 710072, China

[c] Centre of Advanced Materials Processing and Manufacturing, The University of Queensland, St Lucia, QLD 4072, Australia

Abstract: The flow stress behavior of 10 vol. % short carbon fibers reinforced AZ91D composites (C_{sf}/AZ91D) were investigated by hot compression test. The results show the flow stress reach the peak value at small strain and then decrease monotonically until the end of the large strain, which exhibits an obvious dynamic strain softening. The decrease of stress level with deformation temperature increasing or strain rate decreasing can be represented by Zener-Hollomon parameter in a hyperbolic sine equation. By considering the effect of strain on material constants, a modified viscoplastic constitutive equation was established to characterize the dependence of flow stress on the deformation temperature, strain, and strain rate. The stress-strain values calculated by the constitutive equation are in consistent with the experimental results. Applying the constitutive equation, the plastic deformation of C_{sf}/AZ91D

* Corresponding author. Tel: +86-791-86453167; Fax: +86-791-86453167.
E-mail address: wangzhj@nchu.edu.cn.

composites during the hot compression process were analyzed by finite element simulation. The calculated punch force-stroke curves agree well with the measured ones. The results confirmed that the established constitutive equation can accurately describe the hot plastic deformation behavior of C_{sf}/AZ91D composites, and can be used for the finite element analysis on the hot forming process.

Keywords: magnesium matrix composites; hot compression; flow stress; constitutive equation; numerical simulation

1. Introduction

Discontinuous reinforced magnesium matrix composite is an excellent candidate for high-performance and lightweight structural materials, owing to their high specific strength, high dimensional stability, good damping capacity and isotropic properties [1, 2]. However, the cold and hot deformability of this kind of composite is relatively poor because of the hexagonal close-packed crystal structure of magnesium as well as the brittle reinforcements embedded in it [3-5]. During being thermo-mechanical processed, the plastic deformation leads to the rearrangement or breakage of reinforcements as well as the dynamic recrystallization of magnesium [6, 7]. These metallurgical transformations combine to yield a more significant strain softening, i.e. the decline of flow stress with the increase of plastic strain, than that of the magnesium alloy [8-10]. Consequently, the flow stress of magnesium matrix composites is determined not only by the deformation temperature and strain rate but also by the plastic strain largely.

In previous constitutive modeling on hot deformation behavior of metal matrix

composites, the effect of deformation temperature and strain rate on flow stress was represented by Zener-Hollomon parameter [11, 12]. By introducing this parameter in a power, exponential or hyperbolic sine type equation, the dependence of peak stress or steady stress on the temperature and strain rate can be expressed [13-16]. However, the relationship between flow stress and strain was not considered adequately in these constitutive models. The strain softening, which is the primary deformation pattern for metal matrix composites, can not be properly characterized. To perform an accurate numerical simulation and optimization of hot forming for metal matrix composites, it is essential to develop a comprehensive constitutive model, in which the combined effect of deformation temperature, strain rate and plastic strain on the flow stress can be formulated properly.

In the present study, the hot deformation behavior of short carbon fibers reinforced magnesium matrix composites (C_{sf}/AZ91D) was investigated by compression test. According to the results, the dependence of flow stress on temperature and strain rate were represented by a hyperbolic sine model. The material constants in this model were identified and expressed as a function of strain by nonlinear regression analysis. Considering the effect of strain on material constants, the influence of strain on flow stress was incorporated in a modified hyperbolic sine constitutive equation, by which the significant strain softening can be formulated during the severe plastic deformation. Furthermore, the validity of the determined constitutive equation was investigated by applying it to the numerical simulation of the hot compression process.

2. Material and experiment

AZ91D alloy reinforced with 10 vol. % chopped carbon fibers (called as C_{sf}/AZ91D composites) were investigated in this study. The composition of the magnesium alloy was 8.30-9.70 wt.% Al, 0.35-1.00 wt.% Zn, 0.15-0.50 wt.% Mn, 0.10 wt.% Si, 0.03 wt.% Cu, balance being Mg. The dimensions of the chopped carbon fibers were 6μm in diameter and 100~200μm in length. The composites were fabricated by the pressure infiltration technique and the detailed procedure of the pressure infiltration can be found in the authors' previous publication [17]. The as-infiltrated composites ingot was cut into cylindrical specimens with the diameter of 8 mm and height of 12 mm. The specimens for hot compression testing were treated by T6 procedure to relax the residual stress aroused during the fabrication and machining process.

The hot compression tests were performed on a Gleeble-1500D thermo-mechanical simulator, with deformation temperature ranging from 596K to 696K, strain rate ranging from $0.005s^{-1}$ to $0.5s^{-1}$ and ultimate compression ratio 50%. In order to reduce the friction between the specimens and crossheads, graphite lubricant was used for the compression tests. All the specimens were firstly heated to the desired deformation temperatures with a heating rate of 10K/s, followed by an isothermal holding time of 180s before compression in order to obtain the heat balance in specimens. A thermocouple element was inserted in the specimen at the middle section. By thermo-coupled feedback-controlled AC current, the temperature of specimens during heating and compression can be controlled.

3. Results and discussion

3.1 Hot deformation behavior

The true stress-strain curves of the C_{sf}/AZ91D and AZ91D compressed at elevated temperature are shown in Fig.1. According to the flow stress curves, it can be found the flow stress decreases with the increase of deformation temperature, whereas it increases as the strain rates increasing. When the C_{sf}/AZ91D composites were hot compressed, the enhancement of fiber result in a sharp stress peak on the flow stress curves at the elevated temperature, as shown in Fig.1 (a)-(c). Under the same deformation conditions, it can be seen the stress peak on the flow stress curve of AZ91D alloy (as shown in Fig.1 (d)) was unapparent as compared to that of the composites.

According to the whole stress-strain curves of the composites in Fig.1, after the flow stress reaches the peak at the small strain, it can be seen that the flow stress decline continuously with the growth of true strain. This indicates the composites undergoing the hot compression exhibit an obvious strain softening behavior. Nevertheless, the dynamic strain softening of the C_{sf}/AZ91D composites (Fig.1 (a)-(c)) is more significant than that of the corresponding magnesium alloy (Fig.1 (d)). For the AZ91D alloy compressed at elevated temperature, the main mechanism of strain softening was the dynamic recrystallization (DRX) [18]. When the composites were compressed, the reinforcement effect of fiber was weakened owing to the breakage of fiber undergoing severe plastic strain, which can be found in Fig.2. As a result, the degree of strain softening in the composites is higher than that in AZ91D alloy, and the stress peak on

the flow stress curves of the composites is sharper in contrast to that of AZ91D. The deflection and fracture of fibers may play a dominant role in contribution to the decrease of flow stress under severe deformation.

3.2 Constitutive equation

The effect of deformation temperature and strain rate on the flow stress can be represented by the Zener-Hollomon parameter synthetically, which can be expressed as following

$$Z = \dot{\varepsilon} \exp(Q / RT) \tag{1}$$

where $\dot{\varepsilon}$ is the strain rate(s^{-1}), Q is the apparent activation energy of hot deformation ($KJ \cdot mol^{-1}$), R is the universal gas constant ($8.31J \cdot mol^{-1} \cdot K^{-1}$) and T is the absolute temperature (K).

During constitutive modeling of hot plastic or creep deformation, the dependence of flow stress on the temperature and strain rate is usually described by the Arrhenius type model [19]. It can also be shown with Zener–Hollomon parameter as given in Eq. (2), (3) and (4). For the low stress level, the power law (Eq. (2)) was preferred, while the exponential law (Eq. (3)) was suitable for expression of the high stress level. For all stress level, the hyperbolic sine model (Eq. (4)) gives better approximations between Zener-Hollomon parameter and stress [15, 16, 20 and 21].

$$Z = \dot{\varepsilon} \exp(Q / RT) = A\sigma^{n'} \tag{2}$$

$$Z = \dot{\varepsilon} \exp(Q / RT) = A \exp(\beta\sigma) \tag{3}$$

$$Z = \dot{\varepsilon} \exp(Q / RT) = A[\sinh(\alpha\sigma)]^{n} \tag{4}$$

where $\beta = \alpha \cdot n'$, σ is the flow stress (MPa). A (s^{-1}), α (MPa^{-1}), n' and n are the material constants at a specific strain.

The material constants in the constitutive equations can be determined using the true stress-strain data obtained from the hot compression tests. Taking logarithm of both sides of Eq. (2), (3) and (4) respectively arrive at

$$\ln \dot{\varepsilon} = n' \ln \sigma + \ln A - Q/RT \tag{5}$$

$$\ln \dot{\varepsilon} = \beta \sigma + \ln A - Q/RT \tag{6}$$

$$\ln(\dot{\varepsilon}) = n \ln[\sinh(\alpha\sigma)] + \ln A - Q/RT \tag{7}$$

At deformation temperature of 646K and 696K, substituting the stress value at a specific strain and the corresponding strain rate into Eq.(5), the value of n' can be calculated from the average slope of the lines in $\ln \dot{\varepsilon} - \ln \sigma$ plots. The lines in $\ln \dot{\varepsilon} - \sigma$ plots can be plotted using the stress value at the specific strain and the corresponding strain rate at temperature of 596K and 646K. Based on Eq.(6), the value of β at the specific strain can be acquired from the average slope of these $\ln \dot{\varepsilon} - \sigma$ lines. Thereafter, the value of α was calculated according to $\beta = \alpha \cdot n'$. At different true strain, the values of n', β and α were calculated and present in Table 1.

At the specific strain, substituting the value of flow stress and the corresponding strain rate into Eq. (7), the value of n can be deduced from the average slopes of the lines in $\ln \dot{\varepsilon} - \ln[\sinh(\alpha\sigma)]$ plots at all temperature level. Using the value of α at different strain (in Tab.1), the value of n varying with true strain can be calculated by repeating the above procedure. At different true strain, the value of n was presented in

Table 2.

At a certain strain rate, re-arranging Eq. (7) and differentiating it with respect to $1/T$ gives,

$$Q = Rn\frac{d\{\ln[\sinh(\alpha\sigma)]\}}{d(1/T)} \quad (8)$$

By substituting the value of α (in Tab.1), n (in Tab.2) and the flow stress at specific strain into Eq. (8), the relation of $\ln[\sinh(\alpha\sigma)]$ versus $1/T$ was plotted. The slope in a plot of $\ln[\sinh(\alpha\sigma)]$- $1/T$ line was used to calculate Q while the intercept give the value of $\ln A$. At the specific strain, both the value of the Q and $\ln A$ was determined by averaging the values of Q and $\ln A$ under different strain rates. Tab.2 gives the value of Q and $\ln A$ calculated at different true strain. It can be seen that the fluctuation of Q with true strain was not prominent as comparing with that of α, n and $\ln A$ in Table 1 and Table 2. Therefore, the value of Q is taken as average of the values obtained at different strains. The apparent activation energy for C_{sf}/AZ91D composites in the hot compression is equal to $205.13\,KJ\cdot mol^{-1}$, which is higher than the value for lattice self-diffusion of pure Mg. However, it is very close to the value of the apparent activation energy of whisker reinforced magnesium composites [10, 22], in which the deformation mechanism is identified as diffusion controlled dislocation climb. In the current study, the mean stress exponent (n=6.7) of the composites is between 5 and 8. According to the reference [23], it can be concluded that the hot deformation mechanism of C_{sf}/AZ91D composites may be dislocation climb creep or dispersion strengthened or the combination of both modes.

In Fig.1, it can be found the flow stress depends largely on the true strain besides on the deformation temperature and strain rate. Therefore, the strain softening effect should be reflected during the constitutive modeling. One approach is to incorporate a strain-related term in the constitutive model that describes the relationship between temperature, strain rate and stress, such as the classical Johnson-Cook model [24]. Generally, this kind of model is suitable to characterize the dynamic mechanical response of material undergoing the ultrahigh or high strain rate. For analyzing the plastic deformation behaviors of DRMMCs or monolithic alloys during hot forming process, the hyperbolic sine model (Eq. (4)) was usually employed [25]. However, this model can hardly describe the hot deformation behavior of the C_{sf}/AZ91D composites reasonably, because the strain softening can not be expressed quantificationally. In the present study, the influence of strain was revealed by defining the material constants in Eq. (4) as the function of true strain. To find a suitable equation which can properly depict the value of α, n and A varying with the true strain, several types of equation including polynomial and power function were tried and tested. It was found the relationship between these material constants and the true strain can be described with very good correlation and generalization (as shown in Fig. 3) by the regression equations as following,

$$\begin{cases} \alpha = 0.0130 + 0.0153\varepsilon \\ n = 4.7239 + 14.6391 \cdot \varepsilon^{1.9762} \\ \ln(A) = 29.574 + 100.217 \cdot \varepsilon^{2.3695} \end{cases} \tag{9}$$

At a particular deformation condition (i.e. temperature and strain rate), the flow

stress of C_{sf}/AZ91D composites at different true strain can be calculated by the following equations,

$$\begin{cases} \sigma = \frac{1}{\alpha}[\sinh^{-1}(\frac{Z}{A})^{\frac{1}{n}}] \\ Z = \dot{\varepsilon}\exp(\frac{205.13\times10^3}{RT}) \end{cases} \quad (10)$$

where α, n and A can be evaluated by Eq. (9).

Fig.4 shows the comparison of the predicted data by Eq.10 with the experimental flow stress curves for the three different strain rates under temperature of 646K and for the four different temperatures under the strain rates of 0.05s^{-1}. It can be found that the calculated flow stress could track the experimental flow stress curves throughout the entire strain range (0.05~0.6). Almost similar prediction accuracy has also been obtained at other temperature and strain rate levels. The only notable variation between experimental and predicted flow stress data could be observed at the processing condition (in the strain rate of 0.05 $s^{-1}$and temperature of 696K), as shown in Fig.4b. The underestimate of flow stress at 696K may be due to that the outflow of the liquid phase under large strain during the hot compression test. When the composite was compressed near the initial melting temperature of matrix, it has been suggested that a small amount of interstitial liquid tend to flow to outside of the specimen [26]. This may lead to densification of the core in specimen and result in the increase of flow stress. In addition, it was found that this constitutive model failed to describe the elastic stress-strain behavior at very small strain (less than 0.05 in Fig.4). Nevertheless, this model is still feasible for characterizing the flow behavior of the composites during the

hot forming process because the elastic deformation is usually neglected in the numerical analysis on the hot plastic deformation process.

3.3 Validation of the constitutive equation

It can be easily found that the established constitutive equation can give an accurate estimation of the flow stress for C_{sf}/AZ91D composites during the hot compression. However, the rationality of the constitutive equation depends not only on the accuracy of description on flow stress but also on the feasibility and reliability in numerical simulation. Applying the constitutive equation into the finite element simulation of the hot compression, the validity of the derived constitutive equation was further investigated.

Fig.5 shows the geometric model for finite element analysis of the hot compression test. The billet represent the C_{sf}/AZ91D composites being tested and was defined as deformable body. The punch of the thermo-mechanical simulator was defined as rigid isothermal plate. The feed velocity of punch should be reduced in the way of exponential to realize a constant strain rate compression. According to the loading condition in the hot compression test, the feed velocity was calculated and defined by the function as following,

$$\begin{cases} v_1 = 6\times10^{-5}\exp(-t/200), t_1 \in [0,138.6] \\ v_2 = 6\times10^{-4}\exp(-t/20), t_2 \in [0,13.86] \\ v_3 = 6\times10^{-3}\exp(-t/2), t_3 \in [0,1.386] \end{cases} \tag{11}$$

where $v_i (i=1,2,3)$ is the feed velocity of the punch and $t_i (i=1,2,3)$ is the total time for hot compression test corresponding to the constant strain rate of 0.005 s^{-1}, 0.05

$s^{-1}$and 0.5 s^{-1} respectively.

The deformation constitution equation for C_{sf}/AZ91D composites (Eq.10) and the feed velocity of the punch (Eq.11) was introduced in the MSC. Marc software package. The flow behaviors of the C_{sf}/AZ91D composites undergoing the hot compression were numerically simulated by using thermo-mechanical coupled finite element method. Fig.6a shows the distribution of equivalent stress in the billet compressed at the temperature of 646K and the strain rate of 0.05s^{-1}. Fig.6b gives the equivalent stress of point A (as shown in Fig.6 (a) versus time during the hot compression test. It can be seen that the equivalent stress calculated approach to the value of flow stress. The fluctuation on the curve calculated may be caused by mesh distortion and automatic remeshing during the FEM simulation. In general, the variation of equivalent stress calculated can track the true stress-strain curve in the whole process. This indicates the results simulated can reveal the deformation behavior of the C_{sf}/AZ91D composites during the hot compression test.

At different strain rate and temperature, the punch force varying with stroke during the hot compression tests was calculated by the FEM analysis based on the developed constitutive equation. Fig.7 (a) gives the comparison of force-stroke data calculated with the experimental ones at the strain rate of 0.05s^{-1} and the temperature of 596K, 646K and 696K. It can be seen that the calculated stroke force matches the measured one well in the whole hot compression process. At the constant compression temperature (646K), the punch force varying with stroke was calculated at different

strain rates, as shown in Fig.7 (b). It can be observed that the differences between the predicted and measured compression force are inconspicuous at the low strain rate level. The computation error at the strain rate of $0.5s^{-1}$ in Fig.7b is less than 9.6%. This may be caused by the measuring error during the compression test at high strain rate. It is noteworthy that there is an underestimate of the maximum punch force as shown in Fig.6. This may be due to that the composites were assumed to be a rigid-plastic in the current FE analysis and the elastic deformation as the strain less than 0.05 was neglected in the constitutive equation. Beyond that, in the temperature range of 596K~696K and the strain rate range of $0.005\sim0.5s^{-1}$, the comparison of the predicted forming force with the measured one presents a well satisfactory agreement on the whole. This indicates the constitutive equation is valid and reliable in FEM analysis on the current hot forming process for the C_{sf}/AZ91D composites. For the hot forming parameters exceed the current experimental domains, however, the validity of this constitutive model in numerical simulation was not verified and discussed in the present study. In the future, more experiment and FE simulation should be carried out to assess the applicability of the model in far broader hot forming conditions.

4. Conclusions

The hot deformation behaviors of C_{sf}/AZ91D composites were investigated utilizing the hot compression tests. At the given strain, the decrease of flow stress with deformation temperature increasing or strain rate decreasing was represented by a hyperbolic sine equation. A modified viscoplastic equation with its material constants

varying with strain was developed to reveal the strain softening of the composites undergoing severe plastic deformation. The flow stress data predicted by the equation agree with the experimental true stress-strain curve on the whole. This suggested that the constitutive equation can formulate the dependence of flow stress on the deformation temperature, strain rate and strain within the current experimental domain.

By applying the constitutive equation, the deformation of composites during the hot compression tests were simulated and the calculated equivalent stress of center point in the billet approach to the value of flow stress on the whole. It was also found that the calculated force-stoke data of punch can match and track the measured force-stroke curves. The good consistency between the simulation and experiment results confirmed that the current constitutive equation is reliable and feasible for numerical simulation on deformation behavior of the C_{sf}/AZ91D composites during the hot forming process.

Acknowledgement

The authors thank the financial supports from the National Nature Science Foundation of China (No.51365043), the Nature Science Foundation of Jiangxi Province (No.20151BAB206004), the fund of the State Key Laboratory of Solidification Processing in Northwestern Polytechnical University (No. SKLSP201228) and the fund of the National Defense Key Discipline Laboratory of Light Alloy Processing Science and Technology in Nanchang Hangkong University (No. GF201301007). We also thank for the financial support to visiting scholar from the China Scholarship Council (201608360034).

References:

[1] W. L. E. Wong, M. Gupta. Development of Mg/Cu nanocomposites using microwave assisted rapid sintering. Comp Sci Tech 2007; 67(7-8): 1541-52.

[2] W. N. A. W. Muhammad, Z. Sajuri, Y. Mutoh, Y. Miyashita. Microstructure and mechanical properties of magnesium composites prepared by spark plasma sintering technology. J. Alloys Compd 2011; 509: 6021-29.

[3] Y.V.R.K. Prasad, K.P. Rao, M. Gupta. Hot workability and deformation mechanisms in Mg/nano-Al_2O_3 composite. Comp Sci Tech 2009; 69: 1070-76.

[4] Z.J. Li, W.D. Fei, H.Y. Yue, L.D. Wang. Hot deformation behaviors of Bi_2O_3-coated $Al_{18}B_4O_{33}$ whisker reinforced aluminum matrix composite with high formability. Comp Sci Tech 2007,67: 963-73.

[5] J. Liu, L.H. Qi, J.T. Guan, Y.Q. Ma, J.M. Zhou. Compressive behavior of C_{sf}/AZ91D composites by liquid–solid extrusion directly following vacuum infiltration technique. Mater Sci Eng: A 2012;531: 164-70

[6] K.P. Rao, Y.V.R.K. Prasad, C. Dharmendra, N. Hort, K.U. Kainer. Compressive strength and hot deformation behavior of TX32 magnesium alloy with 0.4% Al and 0.4% Si additions. Mater Sci Eng: A 2011; 528: 6964-70.

[7] L. Geng, A.B. Li, Q.Y. Meng. Experimental and numerical studies of the effect of whisker misalignment on the hot compressive deformation behavior of the metal matrix composites. Mater Sci Eng: A 2004; 386: 212-21.

[8] T.W. Gustafson1, P.C. Panda, G. Song, R. Raj. Influence of microstructural scale on

plastic flow behavior of metal matrix composites. Acta Mater 1997;45: 1633-43

[9] V. Sklenicka, M. Svoboda, M. Pahutova, K. Kucharova, T.G. Langdon. Microstructural processes in creep of an AZ 91 magnesium-based composite and its matrix alloy. Mater Sci Eng: A 2001; 319-321: 741-45.

[10] Y.P Zhu, P.P. Jin, P.T. Zhao, J.H. Wang, L. Han, W.D. Fei. Hot deformation behavior of $Mg_2B_2O_5$ whiskers reinforced AZ31B magnesium composite fabricated by stir-casting. Mater Sci Eng: A 2013; 5730:148–53

[11] Z.Y. Ma, S.C. Tjong. Creep deformation characteristics of discontinuously reinforced aluminium-matrix composites. Comp Sci Tech 2001; 61:771-86

[12] I. Tirtoma, M. Guden, H. Yildiz. Simulation of the strain rate sensitive flow behavior of SiC-particulate reinforced aluminum metal matrix composites. Comput Mater Sci . 2008; 42: 570-8

[13] J.S. Marte, S.L. Kampe, A.A. Wereszczak. Elevated temperature deformation behavior of discontinuous reinforced titanium aluminide matrix composites. Mater Sci Eng: A 2003; 346: 292-301

[14] J.M. Zhou, L.H. Qi, G.D. Chen. Research on the constitutive equation of Al_2O_{3sf}/LY12 composite under hot compression deformation. J Plast Eng (in China), 2005;12: 58-62

[15] C.H.J. Davies, E.B. Hawbolt, I.V. Samarasekera , J.K. Brimacombe. Constitutive behaviour of composites of AA6061 and alumina. J. Mater Process Tech 1997; 70: 244-51

[16] S.L. Guo, D.F. Li, D. Chen, H.W. Wang. Flow stress behaviors of in-situ TiB_2/6351 composite during hot compression deformation at elevated temperatures. Trans. Nonferrous Met. Soc. China. 2009; 19: 8-14

[17] L.H. Qi, L.Z. Su, J.M. Zhou, J.T. Guan, X.H. Hou, H.J. Li. Infiltration characteristics of liquid AZ91D alloy into short carbon fiber preform. J Alloys and Comp 2012; 527: 10-5

[18] S.B. Li, Y.Q. Wang, M.Y. Zheng, K. Wu. Dynamic recrystallizati0n of AZ91 magnesium alloy during compression deformation at elevated temperature. Trans. Nonferrous Met. Soc. China 2004; 14: 306-10

[19] C.M. Sellars, W.J. Mctegart. On the mechanism of hot deformation. Acta Metall 1966; 14:1136-8.

[20] H. Takuda, H. Fujimoto, N. Hatta. Modelling on flow stress of Mg-Al-Zn alloys at elevated temperatures. J. Mater. Process. Technol. 1998; 80-81: 513-6.

[21] Z.Q. Sheng, R. Shivpuri. Modeling flow stress of magnesium alloys at elevated temperature. Mater. Sci. Eng. A 2006; 419:202-8.

[22] S.B. Li, M.Y. Zheng, W.M. Gan, K. Wu. Hot deformation behavior of SiC_w/AZ91 magnesium matrix composite and AZ91 alloy. Acta Mater Compo Sinica 2005;22: 103-8

[23] T.G. Nieh, J. Wadsworth, O.D. Sherby. Superplasticity in Metals and Ceramics. Cambridge University Press, New York, 1997.

[24] G. R. Johnson, W. H. Cook. A constitutive model and data for metals subjected to

large strain, high strain rates and high temperatures. In: Proc. 7th Int. Symp. Ballistics, Am. Def. Prep. Org. (ADPA), Netherlands, 1983. 541-8

[25] Y. P. Zhu, P. P. Jin, P. T. Zhao, J. H. Wang, L. Han, W. D. Fei. Hot deformation behavior of $Mg_2B_2O_5$ whiskers reinforced AZ31B magnesium composite fabricated by stir-casting. Mater. Sci. Eng. A 2013; 573: 148-53

[26] L.H. Qi, Z.J. Wang, J.M. Zhou, L.Z. Su, H.J. Li. Constitutive behavior of C_{sf}/AZ91D composites compressed at elevated temperature and containing a small fraction of liquid. Comp Sci Tech 2011; 71(7): 955-61

Table legend:

Table 1. Value of n', β and α derived from different true strain

ε	0.05	0.1	0.2	0.3	0.4	0.5	0.6
n'	6.484	6.281	6.843	8.012	9.662	11.287	14.391
β	0.091	0.094	0.109	0.137	0.178	0.231	0.331
α	0.0140	0.0150	0.0159	0.0171	0.0184	0.0205	0.0230

Table 2. Value of n, Q and $\ln A$ calculated at different true strain

ε	0.05	0.1	0.2	0.3	0.4	0.5	0.6
n	4.931	4.785	5.168	6.131	7.117	8.551	9.992
Q	201.18	175.72	175.22	207.08	239.04	198.98	238.67
$\ln A$	31.554	28.966	30.698	34.967	40.950	50.336	58.742

Figure legend:

Fig. 1 True stress-true strain curves of C_{sf}/AZ91D composite at strain rate $0.005s^{-1}$(a), $0.05\ s^{-1}$ (b), $0.5s^{-1}$ (c) and AZ91D alloy at strain rate $0.5s^{-1}$ (d)

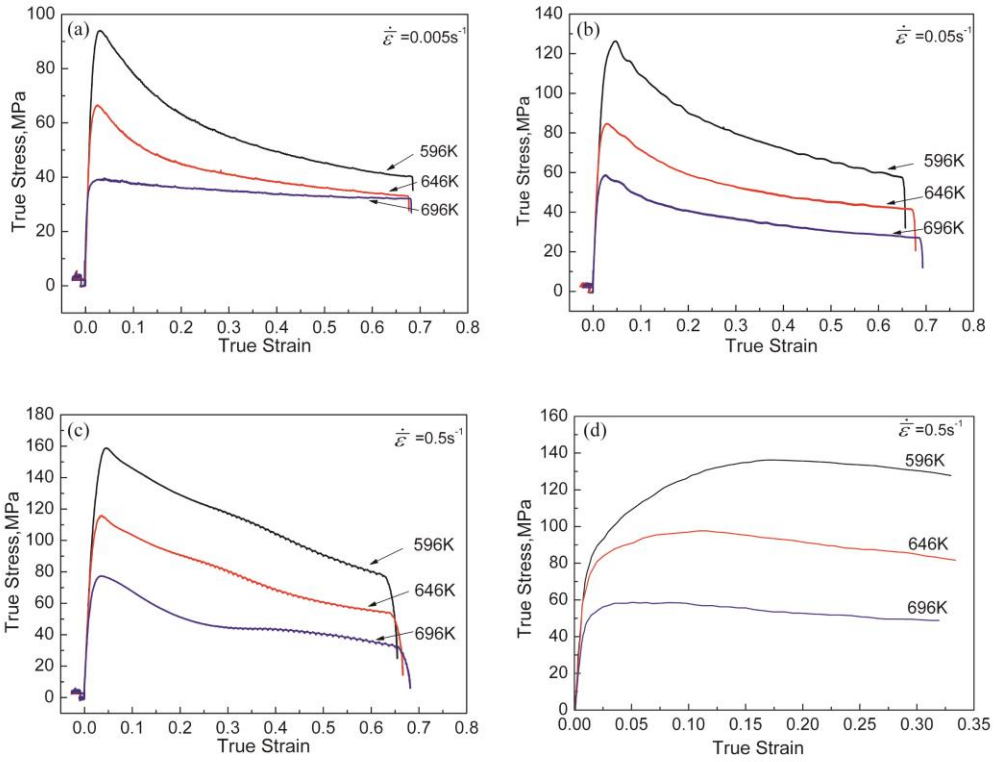

Fig.1

Fig. 2 Morphology of the carbon fiber in the compressed sample (a) and the as-infiltrated composites (b)

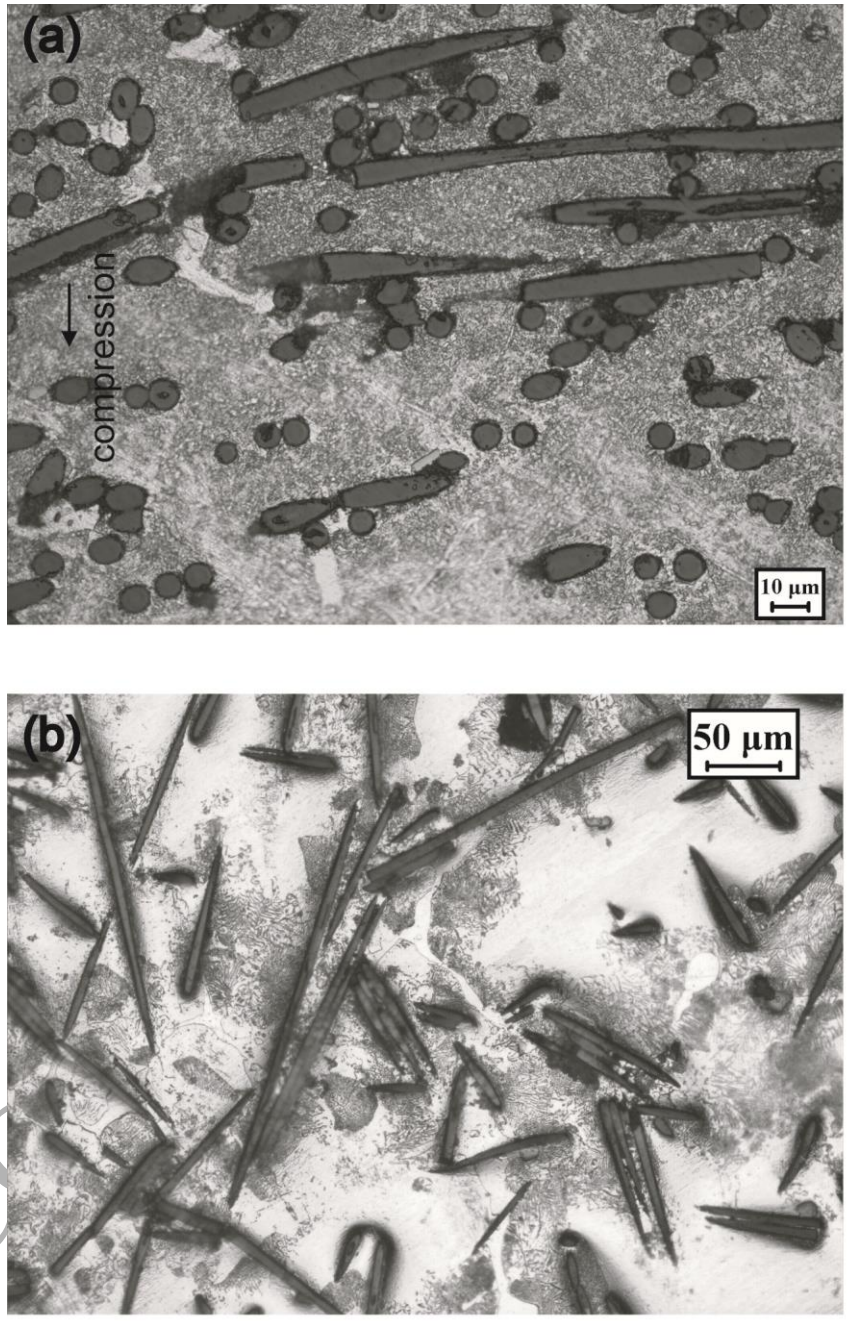

Fig.2

Fig. 3 Fitting curves of (a) α (b) n and (c) $\ln(A)$ versus true strain

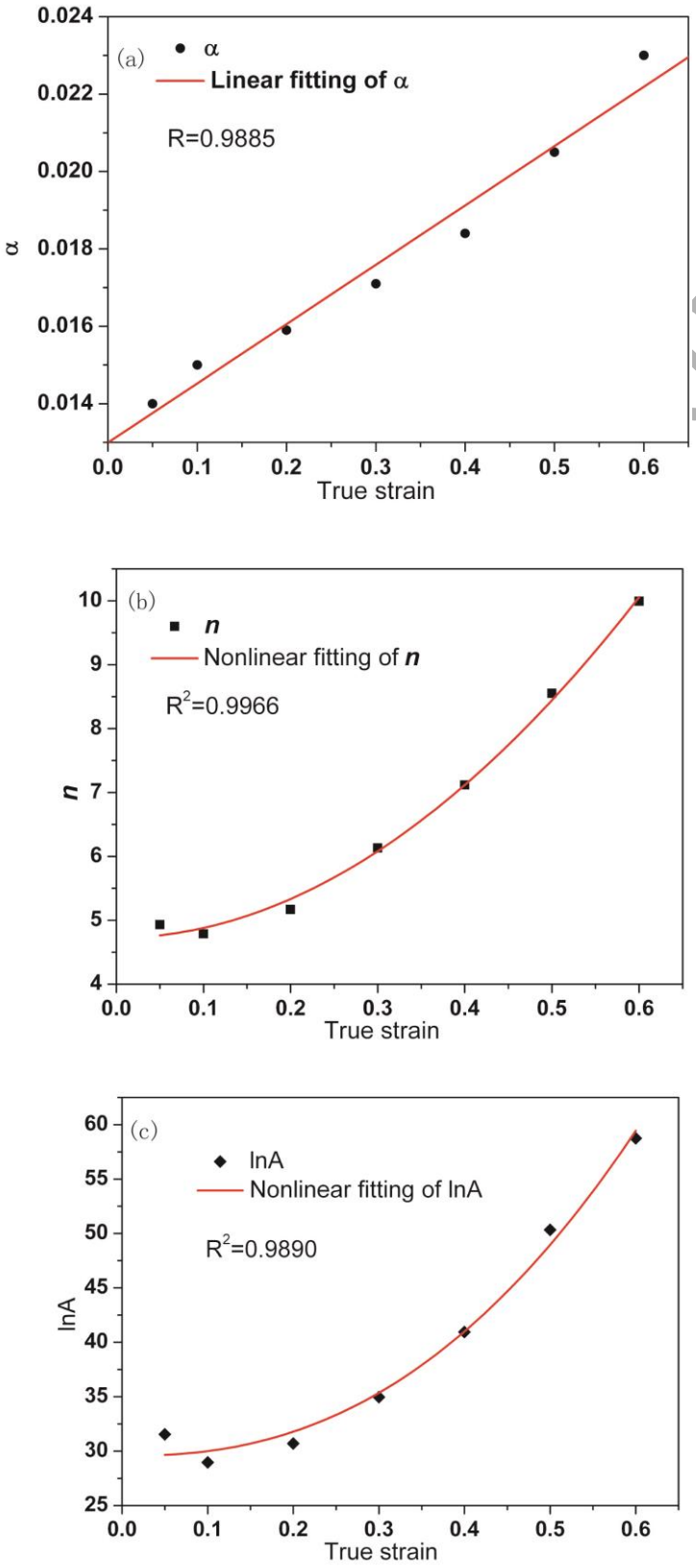

Fig.3

Fig. 4 Comparison of the calculated flow stress data with the measured flow stress curve at temperature of 646K (a) and at strain rate of $0.05s^{-1}$(b).

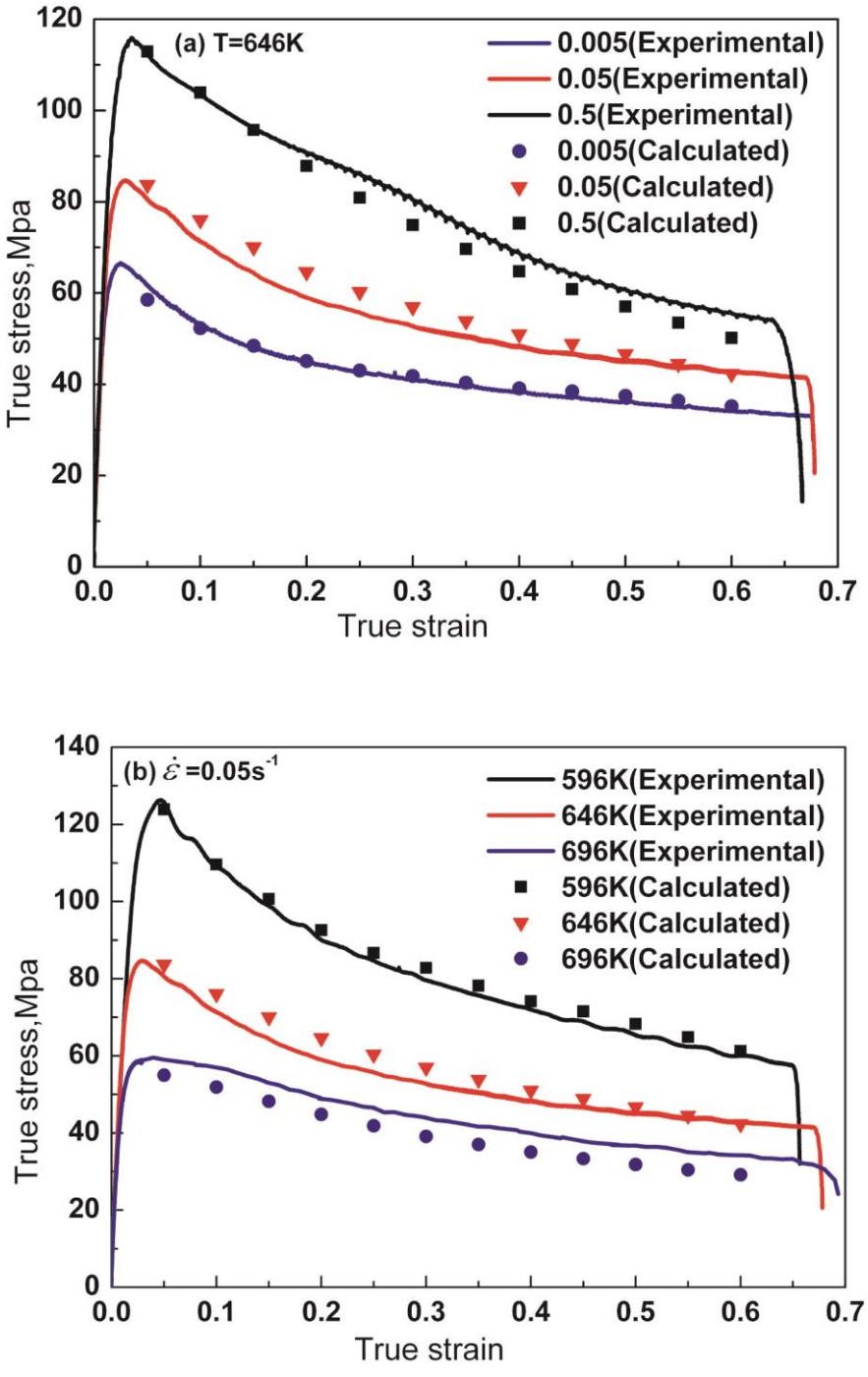

Fig.4

Fig. 5 Geometric model for FEM simulation of the hot compression

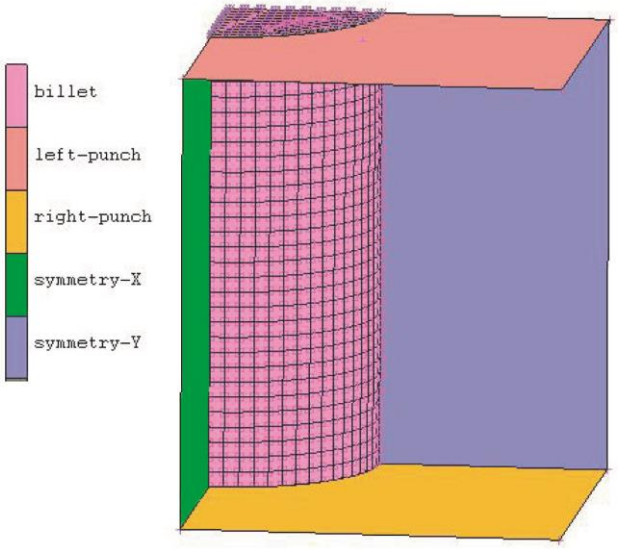

Fig.5

Fig. 6 Equivalent stress calculated by FEM for the hot compression test (a) Equivalent stress of sample calculated at 13s, (b) Equivalent stress calculated (point A) versus true flow stress.

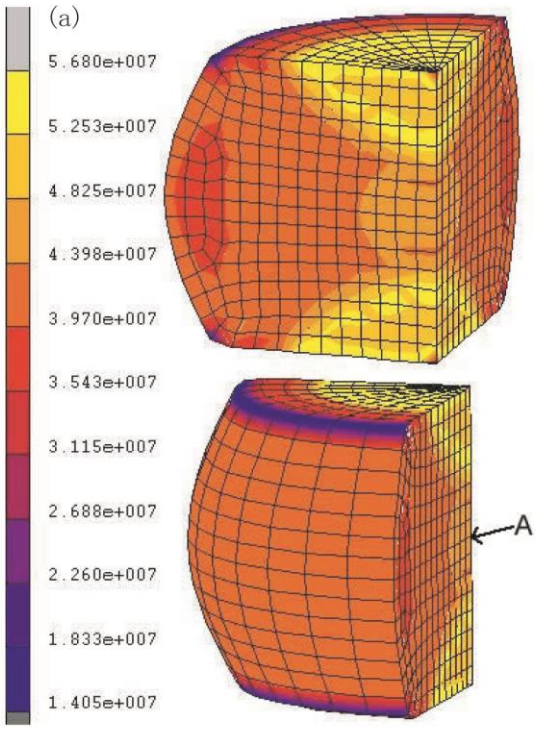

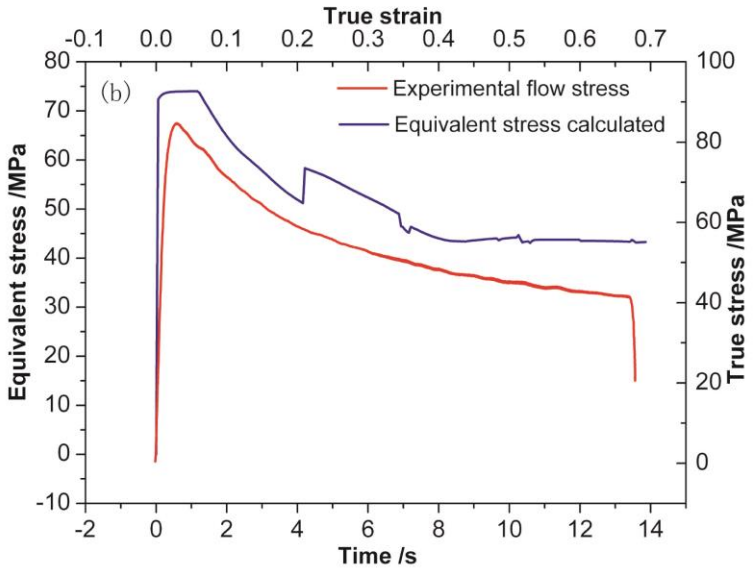

Fig.6

Fig. 7 Calculated and the measured force-stroke curves of the hot compression test (a) at strain rate of $0.05s^{-1}$ (b) at temperature of 646K.

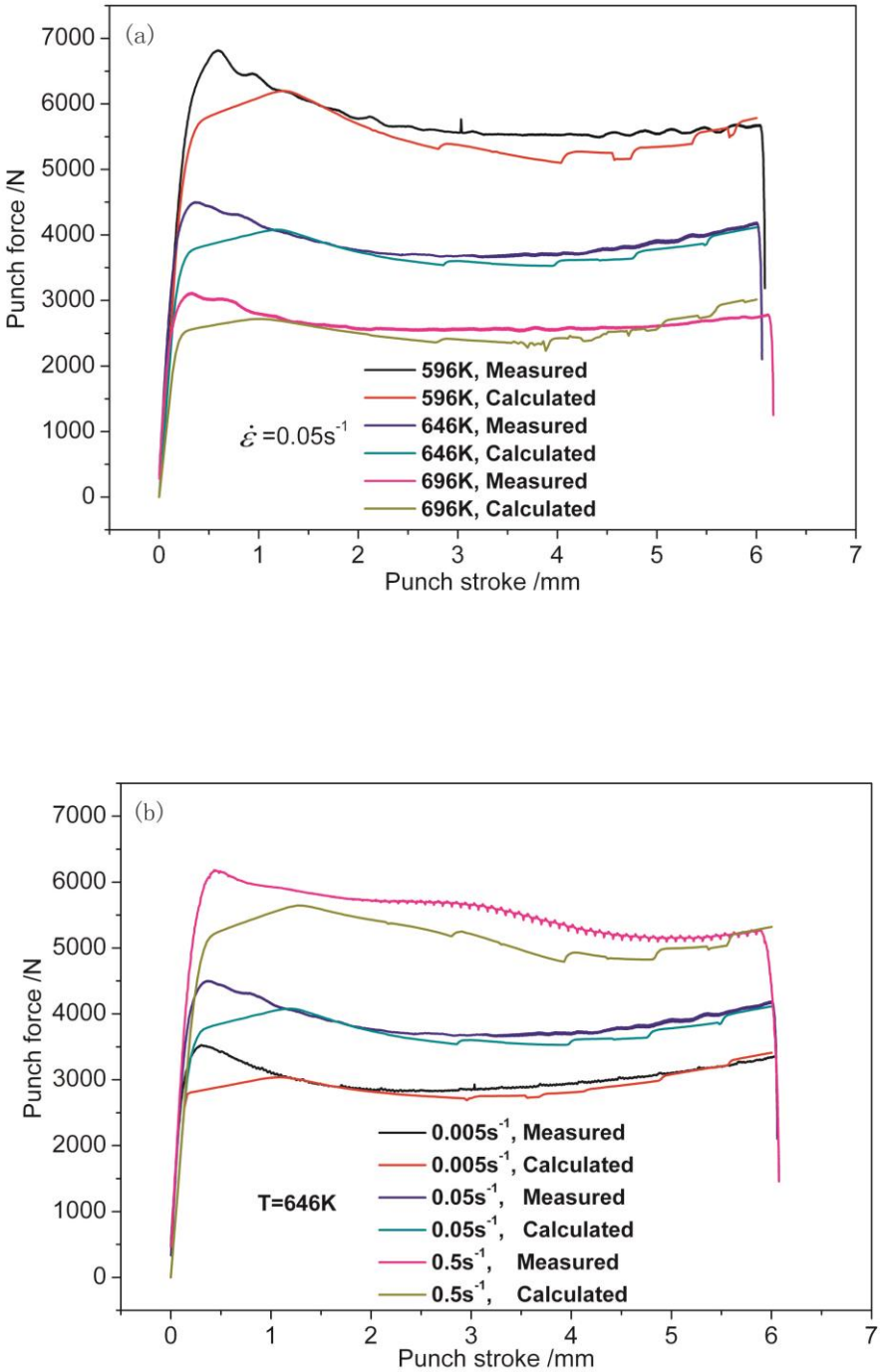

Fig.7